LBL-33755
UC-414
Preprint

Lawrence Berkeley Laboratory
UNIVERSITY OF CALIFORNIA

Accelerator & Fusion
Research Division

Submitted to Journal of Applied Physics

An Efficient Microwave Power Source: Free-Electron Laser Afterburner

C. Wang and A.M. Sessler

March 1993

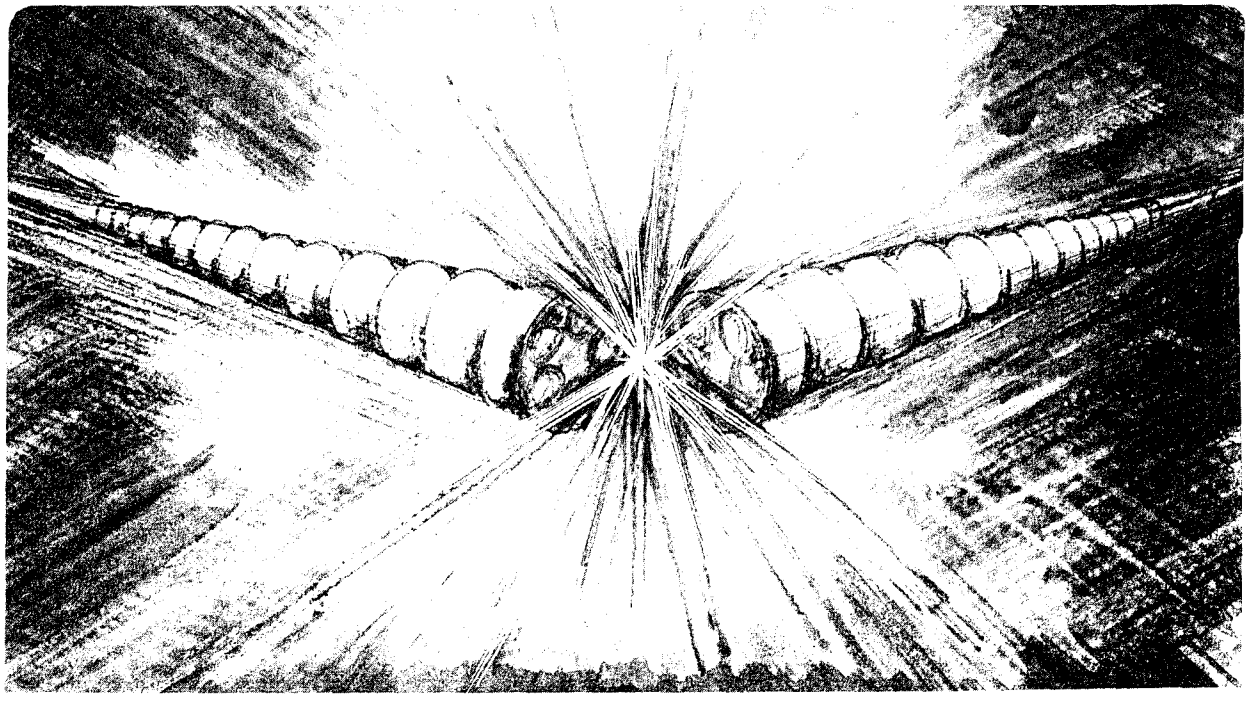

Prepared for the U.S. Department of Energy under Contract Number DE-AC03-76SF00098

LBL-33755
CBP-4
UC-414

An Efficient Microwave Power Source: Free-electron Laser Afterburner*

Changbiao Wang and Andrew M. Sessler

Lawrence Berkeley Laboratory, University of California, Berkeley, California 94720

March 4, 1993

*Work supported by the Director, Office of Energy Research, Office of High Energy and Nuclear Physics, Division of High Energy Physics, of the U.S. Department of Energy under Contract No. DE-AC03-76SF00098

AN EFFICIENT MICROWAVE POWER SOURCE: FREE-ELECTRON LASER AFTERBURNER*

Changbiao Wang[a] and Andrew M. Sessler

Accelerator and Fusion Research Division, Lawrence Berkeley Laboratory

University of California, Berkeley, California 94720

March 4, 1993

A kind of microwave power source, called a free-electron laser afterburner (FEL afterburner) which consists of a free-electron laser buncher and a slow-wave output structure sharing a magnetic wiggler field with the buncher, is proposed. The buncher and the slow-wave structure can operate in either a travelling-wave state or a standing-wave state. In the buncher, the wiggler field together with the radiation field makes an electron beam bunched, and in the slow-wave structure the wiggler field keeps the beam bunched while the bunched beam interacts strongly with the slow-wave structure and so produces rf power. The bunching process comes from the free-electron laser mechanism and the generating process of rf power is in a slow-wave structure. A three-dimensional, time-dependent code is used to simulate a particular standing-wave FEL afterburner and it is shown that rf power of up to 1.57 GW can be obtained, at 17.12 GHz, from a 1-kA, 5-MeV electron beam.

* Work supported by the Director, Office of Energy Research, Office of High Energy and Nuclear Physics, Division of High Energy Physics, of the U.S. Department of Energy under Contract No. DE-AC03-76SF00098.

I INTRODUCTION

A number of methods have been developed for producing a concentration of charge into bunches, and then using these bunches to generate intense coherent microwave radiation. A relativistic klystron[1] achieves bunching by interaction with a longitudinal electric field, while the choppertron[2,3] achieves bunching by interaction with a transverse field in the presence of a collimator. The free-electron laser (FEL) is a high power generator[4] and it is also a good buncher which spacially partitions an electron beam into many small bunches separated by approximately the waveguide wavelength. Shay and his co-workers, and Barletta and his co-workers, studied the FEL buncher and proposed use of the bunched beam for generation of rf power in a two beam accelerator[5] and, also, as an X-ray source in reasearch on biology and material science.[6] Jong and his co-workers proposed the relativistic klystron "afterburner" (RK afterburner) to extract power from a spent FEL electron beam and increase the overall system efficiency.[7] Klystrons consisting of a FEL buncher and a fast-wave radiator, usually called FEL optical klystron,[8,9] multicomponent wiggler FEL,[10] or klystron-type FEL,[11,12] have been extensively studied. In these versions of FEL klystron, unlike the RK afterburner,[7] bunching and radiating processes result from the same FEL mechanism.

In a FEL, the transverse rf current of an electron beam is coherent with the transverse rf electric field, and the beam is bunched in the axial direction by making use of the FEL principle. However, the longitudinal rf current (also called a space charge wave) of the bunched beam is not coherent with the longitudinal rf electric field (if it exists) because the two waves have different phase velocities.[13] If the longitudinal rf current produced by the FEL can become coherent with the longitudinal component of the rf electric field in another structure, then the bunched beam will exchange energy strongly with the rf field in the structure. The free-electron laser afterburner (FEL afterburner) is based upon these considerations.

The FEL afterburner we propose here consists of a fast-wave FEL buncher and a slow-wave structure, as shown in Fig. 1. The FEL buncher and the the slow-wave structure are immersed in the same wiggler magnetic field. When an electron beam travels through the buncher, the longitudinal rf current of the beam has a factor of $\exp\{i(k_{zf}+k_w)z-i\omega t\}$, where k_{zf} is the wave number of the fast-wave buncher and ω is the operating frequency. As is well-known, $\omega/(k_{zf}+k_w)$ is the phase velocity of the pondermotive wave in the FEL buncher. The slow-wave structure is made to have a wave number of $k_{zf}+k_w$, and the same operating frequency as the fast-wave buncher. The electron beam is synchronous with the pondermotive wave, and hence is bunched. The bunched beam is also synchronous with the longitudinal electric field in the slow-wave structure and, hence, intense rf power output will be generated.

In the FEL buncher, the wiggler field together with the FEL radiation field makes the electron beam bunched in the longitudinal direction, and in the slow-wave structure the wiggler field keeps the beam focused and propagating in a bunched form. The main difference between the FEL afterburner and the RK afterburner proposed by Jong et al.[7] is that the slow-wave output structure of the FEL afterburner shares a wiggler field with the FEL buncher, whereas the output cavity of the RK afterbuner does not have a wiggler field. The wiggler field keeps the beam bunched so that, especially at low energies, the FEL afterburner can be very efficient.

Usually, since only the forward wave is synchronous with the electron beam in the FEL buncher, in princple it can operate in a travelling-wave state as well as a standing-wave state. For an over-mode buncher, operation in the travelling-wave state (FEL amplifier mode) has to avoid (usually unwanted) multi-mode competion, while operation in the standing-wave state (FEL oscillator mode) decreases the number of transverse modes because the radiation wave has to fulfil an additional cavity-resonance condition. For a standing-wave buncher, a multi-cavity construction can be employed to enhance beam bunching.

Similarly, a slow-wave structure also can operate in a travelling-wave state or a standing-wave state. Hence the FEL afterburner can operate in a travelling-wave (travelling-wave-to-travelling-wave) state, a standing-wave (standing-wave-to-standing-wave) state, or a mixed state. To enhance rf output power, a multi-cavity construction in the slow-wave output structure also can be used. Experience suggests that a travelling-wave structure is advantageous in practice.

As a specific example, in this work, we present simulation analysis of a particular standing-wave FEL afterburner with a three-dimensional, time-dependent code. In this example, both the FEL buncher and the slow-wave structure operate in a standing-wave state. In section 2, the calculational model of the particular standing-wave FEL afterburner is described. Simulation results are given in section 3, and finally, some conclusions are drawn in section 4.

II DESCRIPTION OF A PARTICULAR STANDING-WAVE FEL AFTERBURNER

As shown in Fig. 2, the buncher of the particular standing-wave FEL afterburner, followed by a slow-wave structure which only has one slow-wave cavity, has three identical cavities operating at 17.12 GHz. We assume that only the $TE_{1,1,91}$ mode is dominant in the cavities. To shorten the start-up time, we input a small power in the first cavity. There are four drift tubes and they have the same radius. These drift tubes provide passage for an electron beam immersed in a combined wiggler magnetic field. The drift tubes are beyond cutoff. We assume that we have set metal meshes at the ends of each cavity to block electromagnetic waves. The length of the fourth drift tube between the third cavity and the fourth cavity (slow-wave cavity) can be changed to adjust the matching of the bunched beam with the slow-wave cavity. In the first drift region, we use seven tapered magnetic wiggler periods to make the electron beam move in helical orbits. In the other three drift tubes and four cavities, the wiggler amplitude is uniform.

The combined wiggler magnetic field is expressed by the following analytic formula

$$B_x = T(z)B_{w0}\left[I_0(k_w r)\cos(k_w r) + I_2(k_w r)\cos(k_w z - 2\theta)\right] \quad (1)$$

$$B_y = T(z)B_{w0}\left[I_0(k_w r)\sin(k_w r) - I_2(k_w r)\sin(k_w z - 2\theta)\right] \quad (2)$$

$$B_z = -2T(z)B_{w0}I_1(k_w r)\sin(k_w z - \theta) + B_0 \quad (3)$$

where B_{w0} is the wiggler amplitude on the axis, B_0 is the axial uniform magnetic field, the wiggler wave number is given by $k_w=2\pi/\lambda_w$ with λ_w the wiggler period, and the tapering factor is given by $T(z)=z/7\lambda_w$ when $z\leq 7\lambda_w$ and $T(z)=1$ when $z>7\lambda_w$.[14]

When an electron beam goes through the tapered wiggler, its cross-section gradually deviates from the wiggler axis. In the uniform wiggler the cross-section reaches its steady motion around the axis. The cross-section area and shape do not change very much while it moves, as shown in Fig. 3.

To simplify calculation, we assume that only the longitudinal component of the electric field is dominant within the interaction region in the slow-wave cavity and its eigen-mode potential vector can be approximated by

$$A_z = A_0 \cos(k_{zs}z) \quad (4)$$

where $k_{zs}=k_w+k_{zf}$ and A_0 is a normalized factor.

A small part of the rf output power comes from the third cavity and most of it is extracted from the fourth cavity. Changing the quality factor of the third cavity also can change the matching phase of the rf current, resulting in variations of the output power from the fourth cavity. Changing the quality factor of the fourth cavity can cause variations of the pulse shape and magnitude of its output power.

III. SIMULATION RESULTS

The three-dimensional, time-dependent code RKFEL was used to simulate the particular standing-wave FEL aferburner with 1440 computational particles.[14] Parameters used in the simulation are given in table 1. Figure 4 shows the input beam energy and

current versus time. The 40-ns pulse has a 5-ns rise time, 30-ns flat top, and 5-ns fall time.

From representative points in the phase space we can directly examine particle bunching. Figure 5 shows the dependence of the radial coordinate r on the time phase $\phi=\omega t$ for the 35^{th} rf bucket of the electron beam after the FEL buncher or before the slow-wave cavity. From it we can see that the beam is bunched by the FEL buncher and all the electrons have passed the 2.5-cm radius drift tubes. The phase spacing between the two bunches is about 2π. The beam is further bunched but the phase spacing becomes smaller when it is passing through the slow-wave cavity, as shown in Fig. 6.

From the longitudinal rf current, we also can examine the bunching process. The better the beam bunches in a concentrated form, the stronger the rf current is. Figure 7 shows the longitudinal rf current as a function of the axial distance z for the 35^{th} rf bucket of the beam. Before the first cavity (from 0 to 140 cm) there no rf current because of no rf field. From the first cavity on, the rf current gradually increases until it reaches its maximum value in the slow-wave cavity. The maximum rf current is above 1700 A, larger than the input beam current, which indicates that the beam is highly bunched.[15]

Figure 8 shows the dependence of the rf output power of the third cavity on time. The maximum power is 96 MW and the power curve does not reach saturation within the pulse length. Figure 9 shows the fourth-cavity rf output power as a function of time. The maximum power is 1.57 GW, corresponding to an efficiency of 31.4%, and the power curve reaches saturation.

VI. CONCLUSION

A kind of microwave power source, the FEL afterburner, has been proposed. The FEL afterburner employs a free-electron laser as the electron beam buncher and a slow-wave output structure to couple the bunched beam for generation of intense rf radiarion. In the FEL afterburner, bunching process results from the FEL mechanism[5] and the radiating process comes from the coupling of the bunches with a longitudinal field. A three-

dimensional, time-dependent code has been used to simulate a particular FEL afterburner with a standing-wave FEL[16] as the buncher and a slow-wave cavity as the standing-wave output structure. The simulation results show that rf power of up to 1.57 GW with an efficiency of 31.4% has been generated at 17.12 GHz from a 1-kA, 5-MeV electron beam in this particular FEL afterburner. Therefore, the FEL afterburner is a promising candidate rf source for future TeV-class linear colliders.

ACKNOWLEDGMENTS

We wish to thank T. L. Houck and W. A. Barletta for helpful discussions. This work was supported by the Director, Office of Energy Research, Office of High Energy and Nuclear Physics, Division of High Energy Physics, of the U. S. Department of Energy under Contract No. DE-AC03-76SF00098.

REFERENCES

[a] Permanent address: High Energy Electronics Research Institute, University of Electronic Science and Technology of China, Chengdu, Sichuan 610054, China.

[1] A. M. Sessler and S. S. Yu, Phys. Rev. Lett. 58, 2439(1987); M. A. Allen, O. Azuma, R. S. Callin, H. Deruyter, K. R. Eppley, K. S. Fant, W. R. Fowkes, W. B. Herrmannsfeldt, H. A. Hoag, R. F. Koontz, T. L. Lavine, T. G. Lee, G. A. Loew, R. H. Miller, R. B. Palmer, J. M. Paterson, R. D. Ruth, H. D. Schwarz, A. E. Vlieks, J. W. Wang, P. B. Wilson, W. A. Barletta, J. K. Boyd, T. Houck, T. J. Orzechowski, D. S. Prono, R. D. Ryne, G. A. Westenskow, S. S. Yu, D. B. Hopkins, A. M. Sessler, J. Haimson, and B. Mecklenburg, in Proceedings of the 1989 IEEE Particle Accelerator Conference, edited by F. Bennett and J. Kopta (Chicago, IL,1989), p. 1123.

[2] J. Haimson and B. Mecklenburg, in Proceedings of the 1989 IEEE Particle Accelerator Conference, edited by F. Bennett and J. Kopta (Chicago, IL,1989), p. 243.

[3] G. M. Fiorentini, T. L. Houck, and C. Wang, to be published in Proceedings of Intense Microwave Pulses (SPIE, Los Angeles, 1993).

[4] T. J. Orzechowski, B. R. Anderson, J. C. Clark, W. M. Fawley, A. C. Paul, D. Prosnitz, E. T. Scharlemann, S. M. Yarema, D. B. Hopkins, A. M. Sessler, and J. S. Wurtele, Phys. Rev. Lett. 57, 2172 (1986).

[5] H. D. Shay, R. A. Jong, R. D. Ryne, S. S. Yu, and E. T. Scharlemann, Nul. Instr. and Meth. A304, 262 (1991).

[6] W. A. Barletta, R. Bonifacio, and P. Pierini, in Workshop on Fourth Generation Light Sources, edited by M. Cornacchia and H. Winick (Stanford, 1992), p.342.

[7] R. A. Jong, R. D. Ryne, G. A. Westenskow, S. S. Yu, D. B. Hopkins, and A. M. Sessler, Nucl. Instr. and Meth. A296, 776(1990).

[8] B. Girard, Y. Lapierre, J. M. Ortega, C. Bazin, M. Billardon, P. Elleaume, M. Bergher, M. Velghe, and Y. Petroff, Phys. Rev. Lett. 53, 2405 (1984).

[9] A. Gover, A. Friedman, and A. Luccio, Nucl. Instr. and Meth. A259, 163 (1987).

[10]M. Billardon, P. Elleaume, J. M. Ortega, C. Bazin, M. Bergher, M. Velghe, Y. Petroff, D. A. G. Deacon, K. E. Robinson, and J. M. J. Madey, Phys. Rev. Lett. 51, 1652 (1983).

[11]K. Takayama, Phys. Rev. Lett. 63, 516(1989).

[12]A. M. Sessler, E. Sternbach, J. S. Wurtele, Nucl. Instr. and Meth. B40/41, 1064(1989).

[13]P. Sprangle, C. M. Tang, C. W. Roberson, in Laser Handbook, Vol. 6, edited by W. B. Colson, C. Pellegrini, and A. Renieri (North-Holland, 1990), p. 263.

[14]C. Wang and A. M. Sessler, to be published in Proceedings of Intense Microwave Pulses (SPIE, Los Angeles, 1993).

[15]For an ideally-bunched electron beam with an input beam current of I_0, the current can be written as $I(t)=I_0T\Sigma\delta(t\pm nT)$, where $T=2\pi/\omega$ is the period and n=0, 1, 2, 3.... Its Fourier expansion is given by $I(t)=I_0 + 2I_0\cos(\omega t) + 2I_0\cos(2\omega t) + 2I_0\cos(3\omega t) + ...$ The amplitude of the harmonic current is twice the input beam current, and so it is not difficult to understand that the rf current can be larger than the input beam current for a highly-bunched beam. From this it might be an effective means to employ higher harmonics in a highly-bunched beam to interac with rf field and produce mutiple-frequency output power.

[16]A. M. Sessler, D. H. Whittum, J. S. Wurtele, W. M. Sharp, and M. A. Makowski, Nucl. Instr. and Meth. A306, 592(1991).

[17]H. G. Hereward, in Linear Accelerators, edited by P. M. Lapostolle and A. L. Septier (North-Holland, 1970), p. 19.

FIGURE CAPTIONS

Fig. 1. Block diagram of the free-electron laser afterburner. The FEL buncher and the slow-wave structure can operate either in a travelling-wave state or in a standing-wave state. The effective electric field interacting with an electron beam is transverse in the buncher and it is longitudinal in the slow-wave structure.

Fig. 2. The particular free-electron laser afterburner with a standing-wave FEL buncher and a slow-wave output cavity immersed in a combined helical wiggler field.

Fig. 3. Electron distribution on the x-y plane in the wiggler field for a 4-mm radius electron beam. (0) initial distribution, (1) at the beginning of the uniform wiggler, (2) at 0.25 periods, (3) at 0.5 periods, and (4) at 0.75 periods. The beam cross-section moves around the wiggler axis, but its area and shape do not change much.

Fig. 4. Input beam energy (upper curve) and current (lower curve).

Fig. 5. Electron distribution on the r-ϕ plane after the FEL buncher for the 35^{th} rf bucket of electron beam. The beam is bunched and the phase spacing of two bunches is about 2π. All the electrons have passed 2.5-cm radius drift tubes.

Fig. 6. Electron distribution on the r-ϕ plane after the slow-wave cavity for the 35th rf bucket of electron beam. The beam is further bunched but the phase spacing of two bunches becomes smaller.

Fig. 7. Dependence of the longitudinal rf current on axial distance for the 35^{th} rf bucket of electron beam. There is no rf current before the first cavity. The rf current reaches a maximum value of above 1700 A in the fourth cavity.

Fig. 8. rf output power of the third cavity versus time. The maximum power is 96 MW and the power curve does not reach saturation.

Fig. 9. rf output power of the fourth cavity versus time. The maximum power is 1.57 GW and the power curve reaches saturation.

Table 1
Parameters used in the simulation

Wiggler period	20 cm
Wiggler amplitude	3500 Gauss
Axial magnetic field	5100 Gauss
Beam current	1000 A
Beam energy	5 MeV
Drift tube radius	2.5 cm
First drift tube length	140 cm
Second drift tube length	20 cm
Third drift tube length	20 cm
Fourth drift tube length	22 cm
Fast-wave cavity radius	5.71 cm
Fast-wave cavity length	80 cm
Interaction length in slow-wave cavity	80 cm
Input power in first cavity	1 kW
External quality factor	
Cavity 1	300
Cavity 2	300
Cavity 3	120
Cavity 4	30

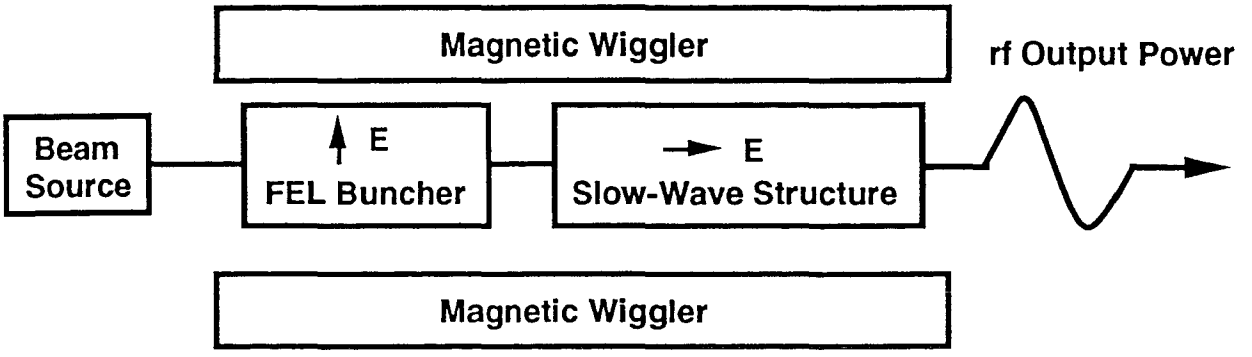
Magnetic Wiggler
rf Output Power
Beam Source
E
FEL Buncher
E
Slow-Wave Structure
Magnetic Wiggler

Fig. 1

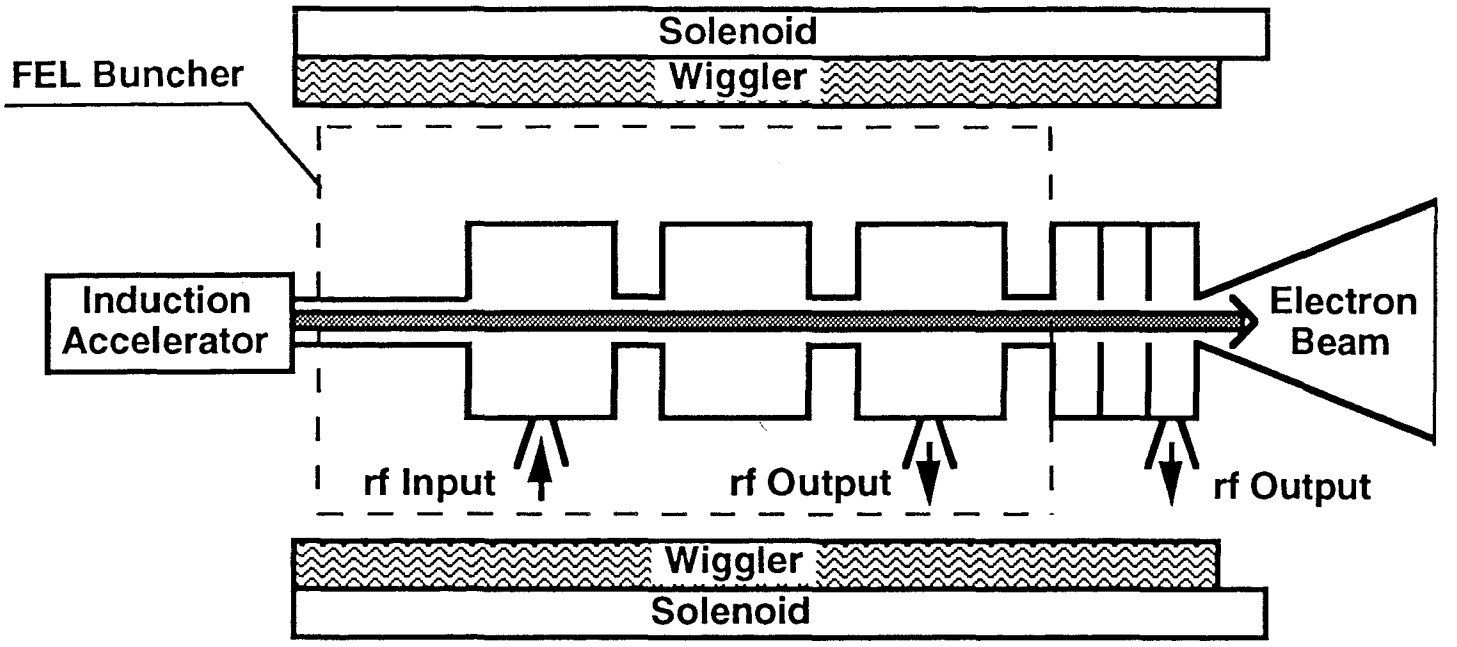
Solenoid
FEL Buncher
Wiggler
Induction
Accelerator
Electron
Beam
rf Input
rf Output
rf Output
Wiggler
Solenoid

Fig. 2

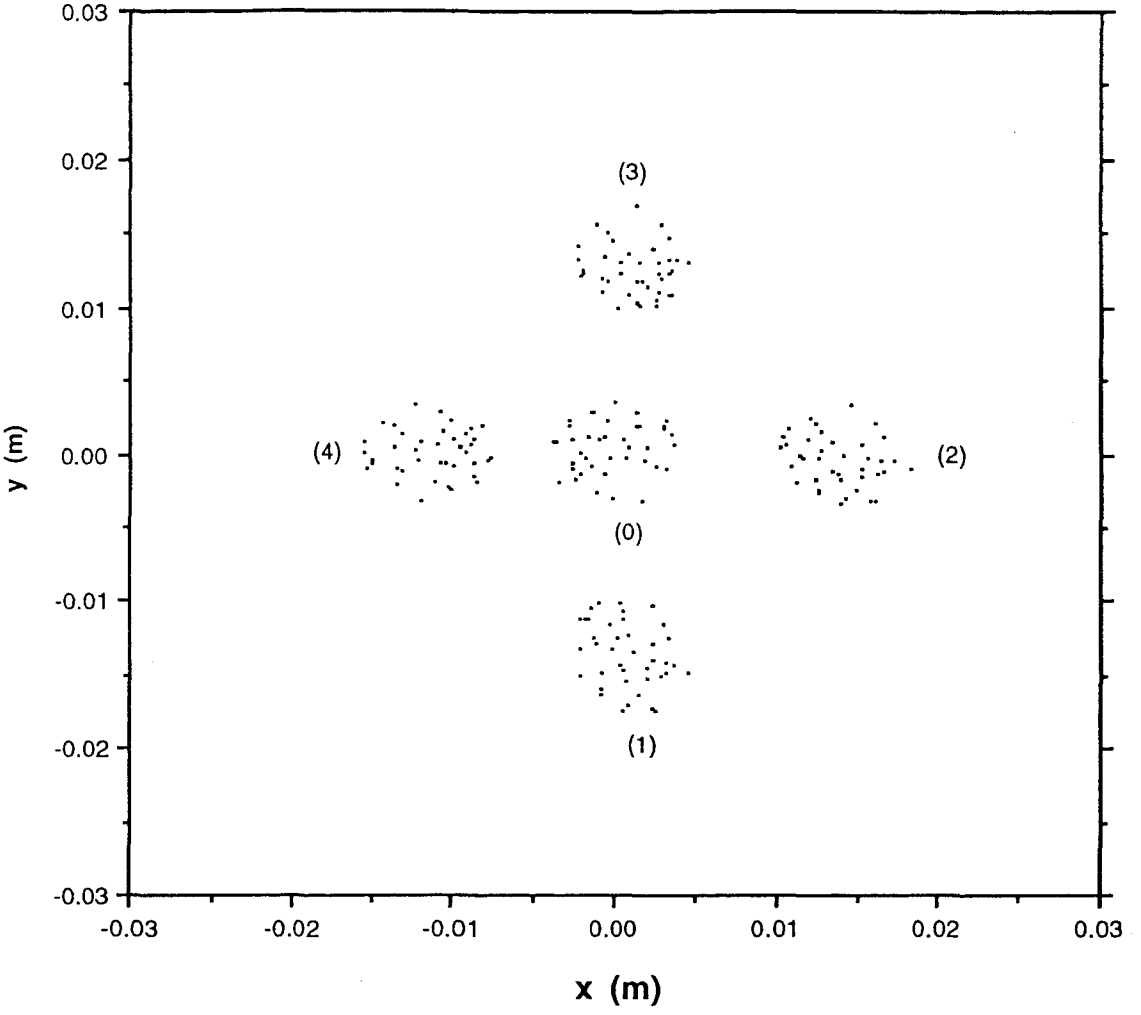
0.03
0.02
0.01
0.00
-0.01
-0.02
-0.03
y (m)
-0.03
-0.02
-0.01
0.00
0.01
0.02
0.03
x (m)
(0)
(1)
(2)
(3)
(4)

Fig. 3

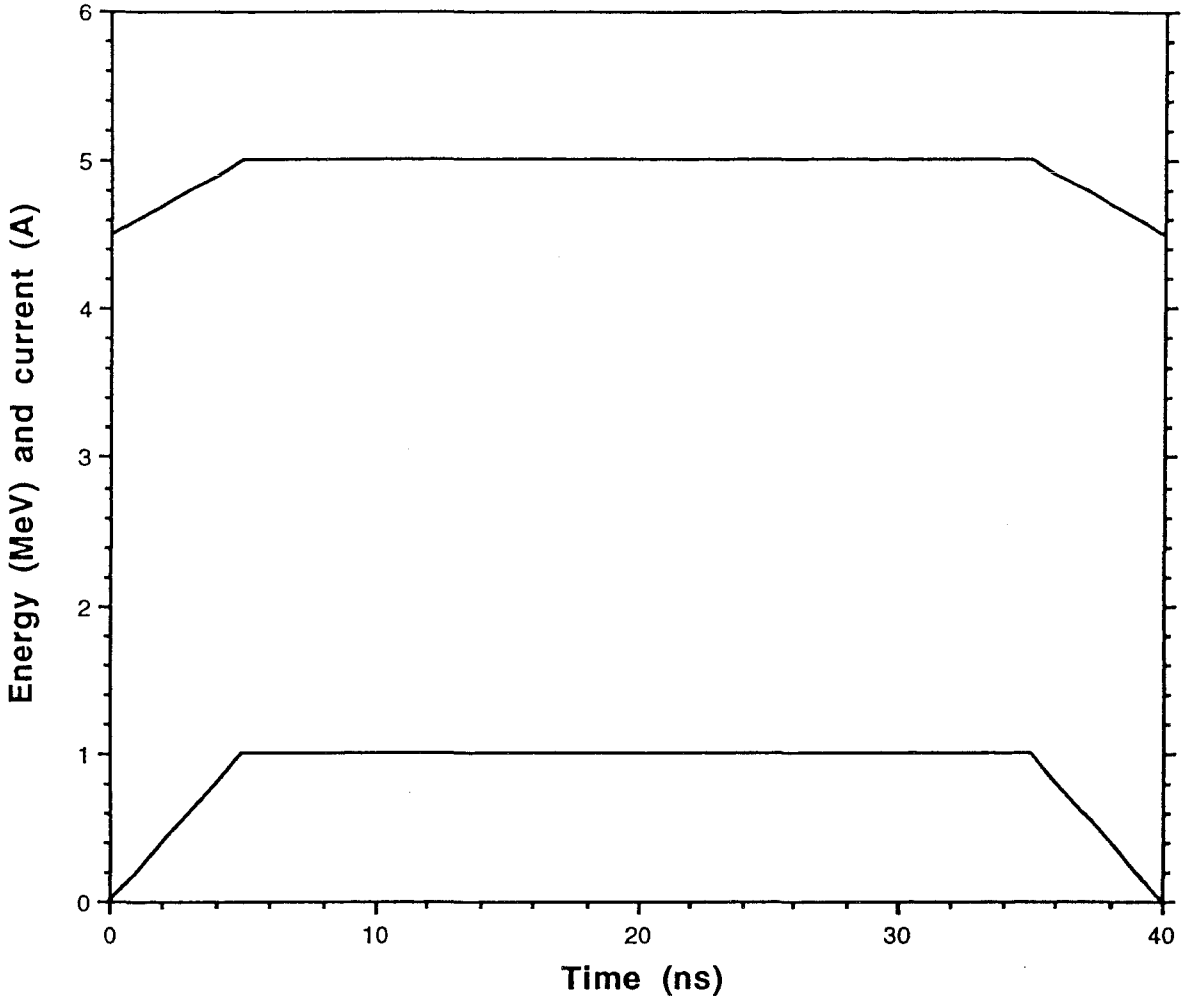

Fig. 4

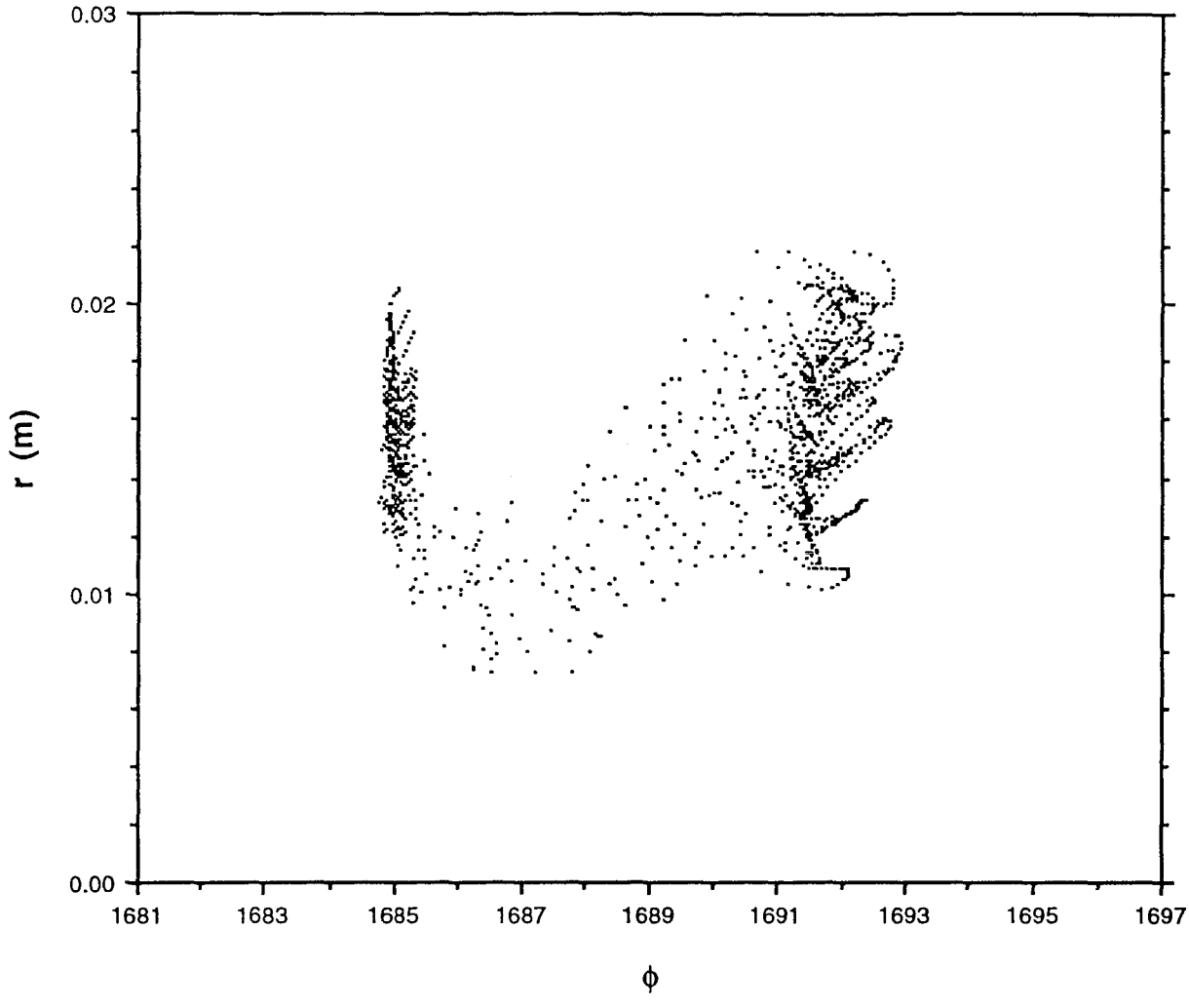
0.03
0.02
0.01
0.00
r (m)
1681
1683
1685
1687
1689
1691
1693
1695
1697
ϕ

Fig. 5

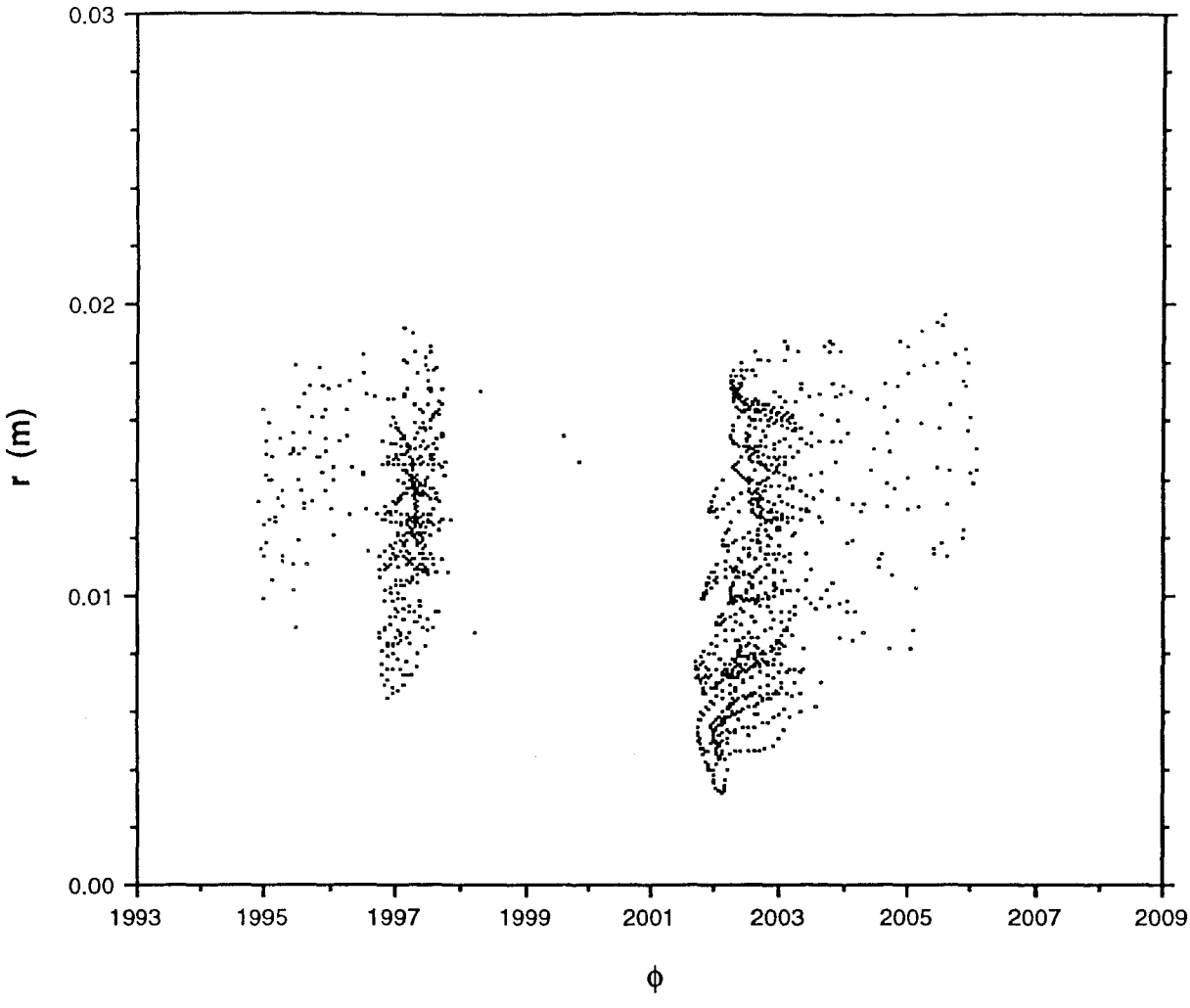
0.03
0.02
0.01
0.00
r (m)
1993
1995
1997
1999
2001
2003
2005
2007
2009
ϕ

Fig. 6

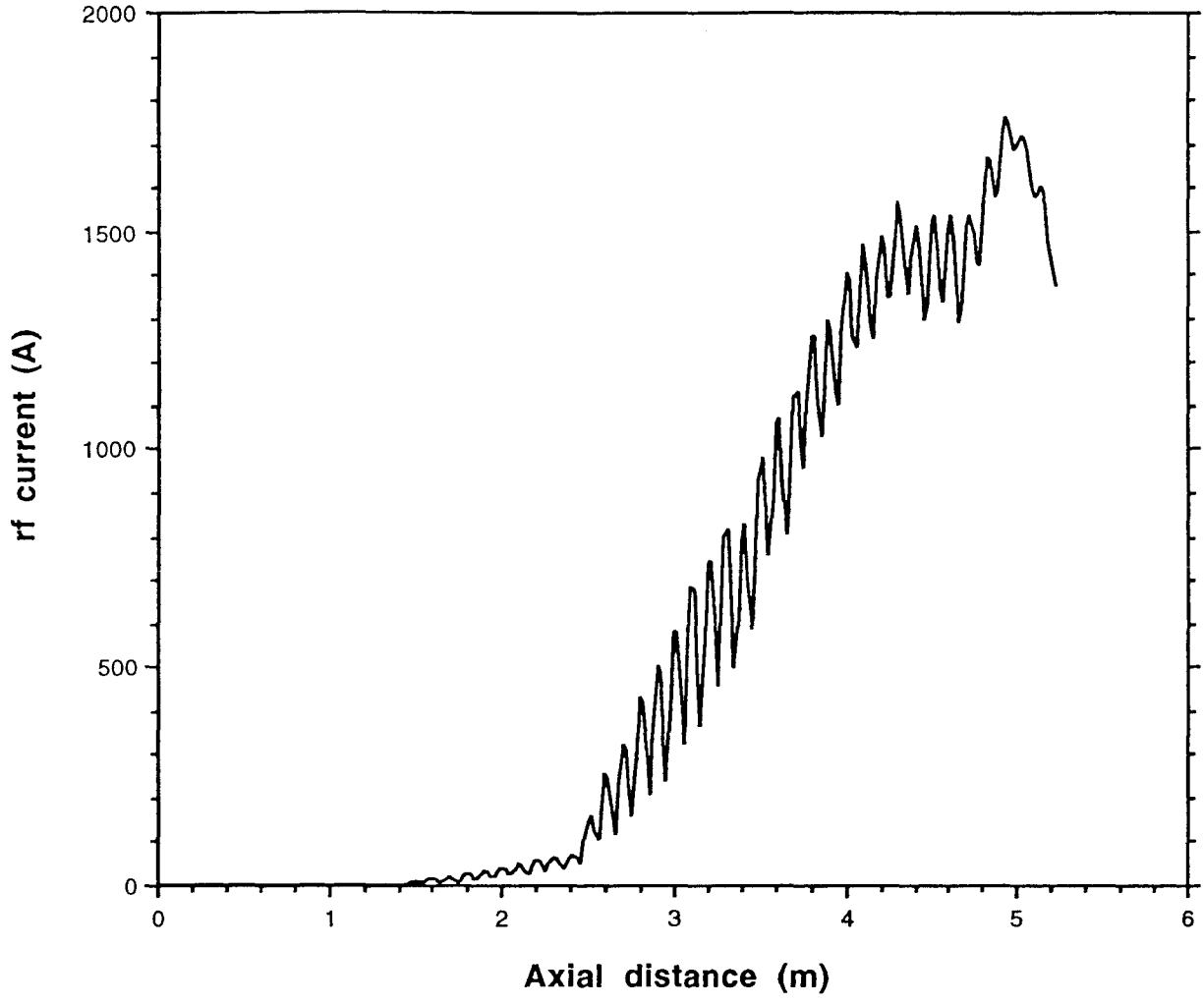

Fig. 7

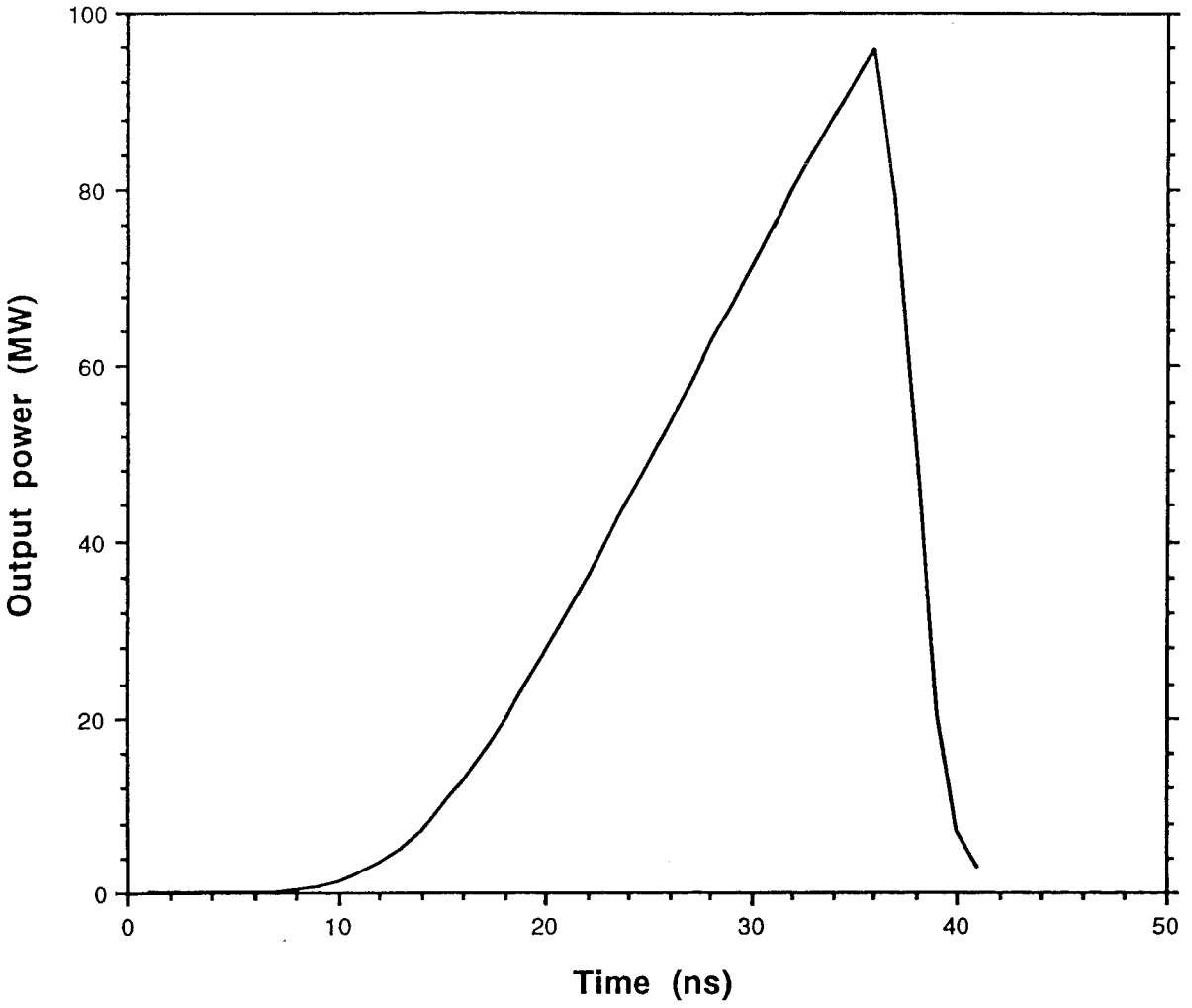

Fig. 8

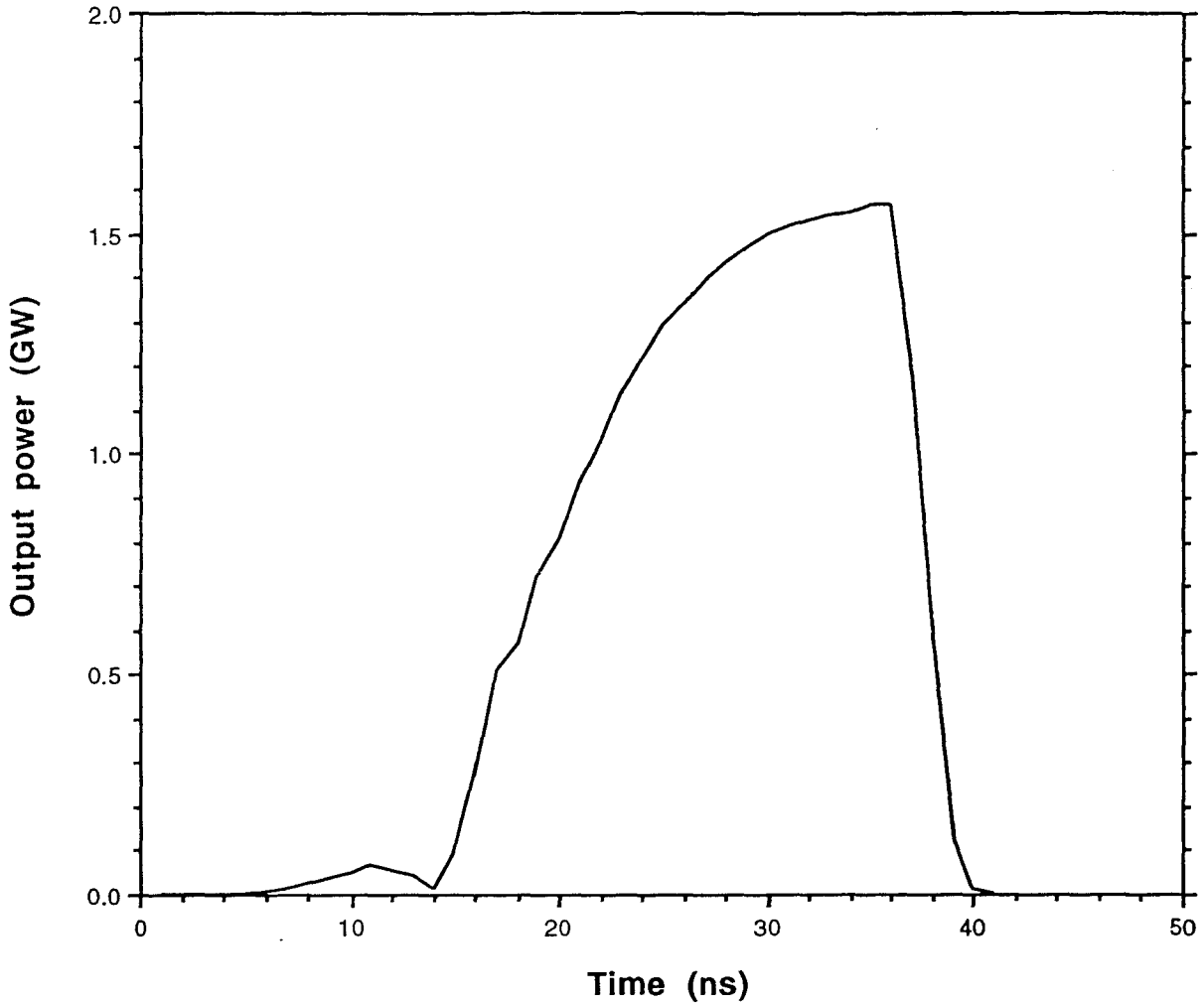

Fig. 9